Int. J. Electrochem. Sci., 11 **(2016)** 10706 – 10714, doi: 10.20964/2016.12.42

International Journal of
ELECTROCHEMICAL
SCIENCE
www.electrochemsci.org

Short Communication

Preparation of Porous Carbon-Manganese Dioxide Nanocomposite as a Supercapacitor Electrode

Yang Ren[1,*], *Chenggong Sun*[2], *Mingjun Song*[1], *Lintong Wang*[1]

[1] College of Chemistry & Chemical and Environmental Engineering, Weifang University, No. 5147 Dongfeng St, Weifang, Shandong, 261061, P.R. China
[2] Shandong Industrial Ceramics Research & Design Institute Co., Ltd., No. 128, Yumin Rd, Zibo, Shandong, 255000, P.R. China
[*]E-mail: renyangwf@163.com

Received: 5 September 2016 / *Accepted:* 4 October 2016 / *Published:* 10 November 2016

Activated porous carbons were prepared from paulownia flower by carbonization and subsequent alkali activation. Then MnO_2-AC_3 composite was synthesized by the electrochemical deposition of manganese oxide nanostructures on the surface of as-prepared activated porous carbons. The MnO_2-AC_3 electrode demonstrates outstanding capacitive behavior with low charge transfer resistance owing to the double layer charge storage and unique pore structure (coexistence of micropores, mesopores and macropores) of activated porous carbons. The stability of MnO_2-AC_3 electrode was affirmed by 1000 successive charge/discharge cycles. The remarkable capacitive behavior and excellent stability make MnO_2-AC_3 promising material with potential application in supercapacitor.

Keywords: Supercapacitor; Activated porous carbon; Manganese oxide; Electrodeposition; Cycle life

1. INTRODUCTION

The exploration of renewable, sustainable and clean energy source is highly demanded owing to the fossil fuel crisis and environment pollution [1, 2]. Supercapacitors (also referred to as electrical double-layer (EDL) capacitors) are recognized as a significant type of energy storage devices due to its fast charging-discharging rate, high power density, safe operation and long cycle life [3-5]. As to the energy output to the electrical facilities, supercapacitors can either be employed directly or coupled with other batteries [6, 7]. In contrast with other secondary batteries, lower energy density is achieved with supercapacitor. Based on the equation $E = CV^2/2$, the energy density can be greatly improved by the effective enhancement of specific capacitance that generally depends on the used electrode

materials. Therefore, various nanomaterials that can be applied as supercapacitor electrodes were extensively studied in order to achieve high capacitance and further high energy output.

The capacitance is greatly affected by the interface area between electrode and electrolyte since the rapid accumulation of charges at the charge interface under an applied electric field is responsible for the charge storage of supercapacitors. Therefore, the electrode materials with remarkably high surface area are highly demanded. Various types of carbon-based materials such as graphene [8-10], carbon nanotubes [11-15] and graphene/carbon nanotube composite materials [16, 17] have been extensively studied as electrode materials because of its very high surface area, good electrical conductivity and outstanding chemical stability against electrolyte. Unfortunately, the industrial application of the above-mentioned carbon-based materials is restricted by the complicated synthesis method with high cost despite of the obtained high capacitance. As an important kind of highly porous carbon materials, activated carbons can be a promising alternative as electrode materials owing to the attractive low cost. Numerous inexpensive and commonly available natural biomass feedstocks such as carbonaceous minerals and biomass wastes can be employed for the preparation of activated carbons by carbonization and subsequent activation with porogens [18, 19]. As to the synthesis of activated carbons as electrode materials in supercapacitors, the employment of various types of raw materials including tea-leaves [20], sunflower seed shell [21], pulps, peels or seeds of fruits [22], porous starch [23], sugar cane bagasse [24] and even pitch [25] have attracted extensive attention nowadays. The capacitance of the obtained activated carbons can be improved by the surface oxygen and nitrogen containing functional groups of biomass precursors [26, 27]. Therefore, rational selection of the biomass precursors with specific surface area, surface functional groups as well as pore structures is very crucial to achieve the activated carbons with optimal capacitance for supercapacitors.

Paulownia flowers that are widely distributed in most regions of China can be employed as precursor for the preparation of activated porous carbon. In most instances, paulownia flower was discarded without effective utilization despite of its good antiviral and antibacterial properties resulted from the active components (e.g., volatile oil and pharmaceutical ingredients) beneath the porous biopolymer texture [28, 29]. Recently, paulownia flower was vigorously explored as biomass precursor for the synthesis of activated carbon owing to its porous texture and various organic components. And the as-prepared activated porous carbon demonstrated high electrochemical performance as electrode material in supercapacitor.

On the other hand, the development of transition metal oxides with low-cot is of great importance as well. Numerous metal oxides such as TiO_2, Fe_3O_4, MnO_2, NiO, VO_x and Co_3O_4 have been extensively studied [30-32]. Among the above-mentioned metal oxides, manganese oxide has been the focus due to many advantages such as low preparation cost and environment friendly [33-35]. As one of the most stable manganese oxides, manganese dioxide has shown remarkable physical properties under ambient conditions with the achieved high capacitance (1370 F/g) of MnO_2-based electrodes in supercapacitor [36]. The capacitance of MnO_2-based electrodes can be further increased with increasing specific surface area through the adoption of a carbon host such as graphite, carbon nanotubes, active carbon and mesoporous carbon [37-40].

Electrochemical deposition is a promising technique for the deposition of MnO_2 nanostructures on the surface of carbon host with controllable structure and thickness by the adjustment of certain

factors such as the applied voltage or current, electrolyte, and temperature during the electrodeposition process [32, 41]. In this study, activated carbons were prepared by dealing biomass precursor paulownia flower with high temperature carbonization and subsequent alkali activation. Then the electrochemical deposition method was employed for the deposition of manganese oxide nanostructures on the as-prepared activated carbon. The supercapacitor fabricated with the manganese oxide/activated porous carbon composite incorporated electrode has demonstrated superior capacitance, good cycling stability and excellent long term stability as well.

2. EXPERIMENTAL

2.1. Chemicals and activated porous carbon synthesis

All chemicals were analytical reagents and used without further purification. Before carbonization, the collected fallen paulownia flowers were firstly washed with deionized water and then dried at room temperature. Subsequently, the clean paulownia flower was transformed to activated carbon through pyrolysis at 800 °C for 2 h under nitrogen atmosphere. The obtained activated carbon was further mixed with KOH with the mass ratio of KOH and activated carbon being 2, 3 or 4, and then the mixture was treated at 800 °C for 1 h under nitrogen atmosphere to create pores. After being cooled to room temperature naturally, the obtained product was washed with 1 M HCl and deionized water until the achievement of neutral pH value. The as-prepared activated porous carbon product was denoted as AC_n (n = 2, 3 or 4 based on the mass ratio of KOH and activated carbon).

2.2. Electrodeposition of manganese oxide

A slurry was firstly prepared by uniformly mixing active materials (85 wt.%), acetylene black (10 wt.%) and polytetrafluoroethylene (5 wt.%) as binder. AC_n electrode was obtained by pouring the slurry onto a clean stainless steel mesh collector. The electrochemical deposition of manganese oxide on AC_n substrate was performed by applying an anodic current of 0.5 mA/cm^2 to mixed solution of manganese acetate (0.1 M) and sodium sulfate (0.1 M) for 30 s at 25 ^oC. Then the MnO_2-AC_n electrode was washed with deionized water several times and annealed at 300 °C for 1 h in the air.

2.3. Electrochemical and BET measurements

The XRD pattern of MnO_2-AC_n electrode was performed on Bruker Advance D8 spectrometer with Cu target. The diffraction patterns were collected in 2θ ranging from 10° to 80°.

For all electrochemical measurements, the three electrode cell containing MnO_2-AC_n working electrode, platinum wire counter electrode and Ag/AgCl reference electrode was employed. Besides, 1 M Na_2SO_4 solution was used as supporting electrolyte. The performance of MnO_2-AC_n electrodes was evaluated through cyclic voltammetry (CV), galvanostatic charge/discharge (CD) and cycle-life stability experiments with the applied potential range 0-1 V at room temperature. In addition, ac-

impedance measurements (EIS) were also performed on Zahner/Zennium potentiostat-galvanostat (Zahner, Germany) under open-circuit potential with AC perturbation amplitude of 10 mV and frequency range from 0.01 Hz to 100 kHz. The specific surface areawas determined by Brunauer EmmetteTeller (BET) method

3. RESULT AND DISCUSSION

Various organic components such as flavonoids, terpenoids, sugar esters, glucosides, sterides and anthraquinones that are enwrapped in thick cell walls of paulownia flower the components can be converted to carbon material by pyrolysis treatment [29]. As can be seen from the XRD patterns (Fig. 1A), a weak and broad diffraction peak at 26° was observed in all AC_n samples. The observed peak can be ascribed to the reflection of (200) lattice plane, indicating the successful carbonization of paulownia flower and synthesis of AC_n samples in low graphitization phase. Another peak corresponds to (101) lattice plane can also be observed after the activation process at higher temperature. The increased crystallinity after the occurrence of (101) lattice is invaluable since the crystallinity is highly correlated with the conductivity which is an important parameter of active electrode material for supercapacitor. The baseline at low angle region was raised owing to the production of micro pores in the carbon framework, suggesting that alkaline treatment was effective not only for the increasement of crystallinity but also for the reinforcement of porous texture. The XRD patterns of MnO_2-AC_n (Fig. 1B) were compared with that of α-MnO_2 (JCPDS 44-0141). It can be observed that the main phase belongs to α-MnO_2. However, certain other phases such as γ-MnO_2 were also existed. According to the Scherrer's equation, the average grain size of MnO_2 was about10 nm.

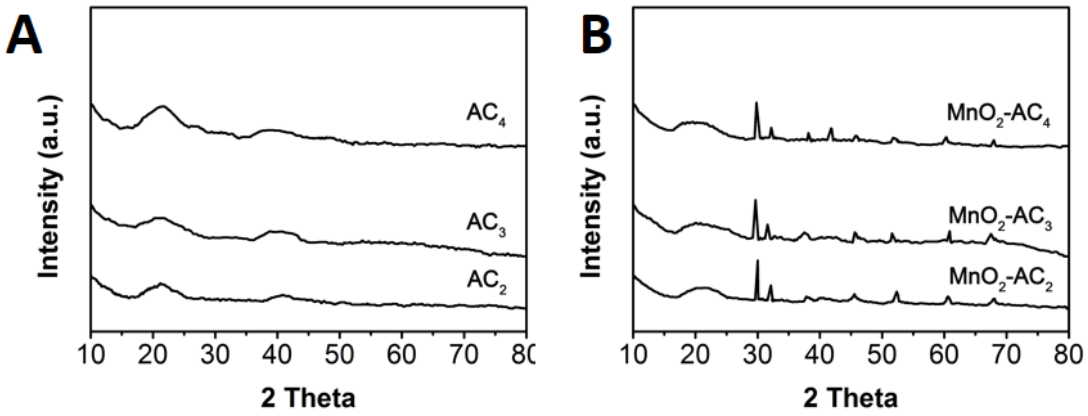

Figure 1. XRD patterns of (A) can and (B) MnO_2-AC_n.

A combined type I/IV nitrogen sorption isotherms based on IUPAC classification were observed for all MnO_2-AC_n composites (Fig. 2). At a relative pressure below 0.1, the adsorption of nitrogen was rapid and distinct, and then at the relative pressure over 0.4, a faint but observable

triangular hysteresis loop could be observed. It can be concluded from the isotherms that a large amount of micropores and a low fraction of interconnected mesopores featured by narrow orifice and large inner cavity were coexisted in the MnO_2-AC_n composites. In addition, the adsorption amount showed a slight increase at the relative pressure near 1, indicating the coexistence of a limit fraction of macropores. The versatile porous texture of MnO_2-AC_n is extremely advantageous for its application as electrode materials in supercapacitor. The high surface area resulted from micropores was very beneficial for the accumulation of electrolyte ions. Besides, the diffusion of electrolyte ions was promoted with shorter diffusion path and less hindrance offered by interconnected meso-/macropores. According to the nitrogen adsorption isotherms, BET surface areas of MnO_2-AC_2, MnO_2-AC_3 and MnO_2-AC_4 were calculated to be 1006, 1159, and 1471 m^2/g, respectively. These result showed a higher values than that of other recent reports biomass carbon [42], nitrogen-doped graphene aerogels [43], spongy nitrogen-doped activated carbonaceous hybrid [44] and nitrogen-functionalized microporous carbon nanoparticles [45].

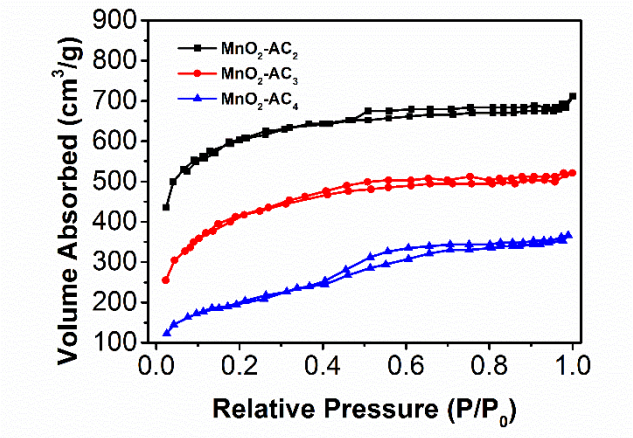

Figure 2. N_2 sorption isotherms of MnO_2-AC_2, MnO_2-AC_3 and MnO_2-AC_4.

Cyclic voltammetry (CV) curves of AC_3, MnO_2-AC_2, MnO_2-AC_3 and MnO_2-AC_4 electrodes were performed in Na_2SO_4 solution at scan rate of 25 mV/s and the results were shown in Fig. 3A. It can be clearly observed that the capacitive current of MnO_2-AC_n was higher than that of AC_n substrate, indicating that the electrochemical performance of AC_n substrate was significantly improved by the deposited MnO_2. The MnO_2 nanostructures play an important role in the enhancement of capacitance by its double layer, indicating the significantly improved capacitance by alkali activation [46]. An approximate ideal capacitor was constructed as demonstrated by the rectangular shape of recorded voltammograms. Moreover, best capacitor performance was achieved with MnO_2-AC_3 as can be seen from its highest voltammograms.

Cyclic voltammetry (CV) curves of MnO_2-AC_3 supercapacitor at different scan rates ranging from 10 to 200 mV/s were performed and the results were shown in Fig. 3B. It was found that the plateau current increased with increasing scan rate. The redox peaks with quasi-rectanglar shape can be maintained with little distortion when the scan rate increased up to 200 mV/s, suggesting the excellent

transport capability of electrolyte ions with fast diffusion kinetics owing to the low inner resistance. The specific capacitance of MnO_2-AC_3 capacitor can be estimated from galvanostatic chargingdischarging curves. Within current densities of 0.5 to 10 A/g, the charging-discharging curves all show symmetric triangular shape with linear voltage vs time profile [47], indicates the overwhelming EDL feature, almost no pesudocapacitance could be discerned in the discharge branches owing to the limited contribution to overall capacitance. The 100% coulombic efficiency featured by the identical charging and discharging duration also evidences the ideal EDL capacitive characteristics of the device. The voltage drop at the beginning of discharge stage originating from IR is negligible at current density below 1 A/g, whereas increases gradually at higher current densities, indicates the increased IR at higher current densities owing to the limited electrolyte diffusion kinetics.

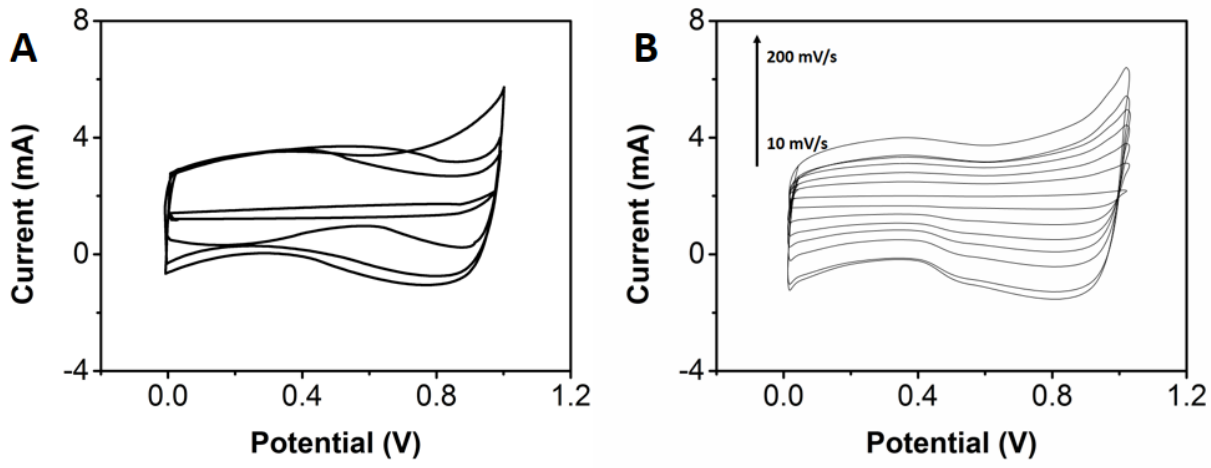

Figure 3. (A) CV curves obtained on AC_3, MnO_2-AC_2, MnO_2-AC_3 and MnO_2-AC_4 electrodes. (B) CV curves of MnO_2-AC_3 supercapacitor at differential scan rates.

Electrochemical impedance spectroscopy (EIS) of MnO_2-AC_3 supercapacitor was performed in Na_2SO_4 solution in order to investigate the charge transfer resistance. As can be seen from Fig. 4A, the impedance plot was composed of nearly vertical line at low-frequency region as an indicator of ideal capacitor and small semicircle at high-frequency region as an indicator of low charge transfer resistance at the interface between MnO_2-AC_3 electrode and electrolyte. The observed low charge transfer resistance makes MnO_2-AC_3 a promising electrode material for high-rate power sources.

Galvanostatic charge/discharge curves for MnO_2-AC_3 electrode was also performed at the current density of 5 A/g and the result were shown in Fig. 4B. The charge/discharge curves were observed to be linear, demonstrating the good capacitive behavior of MnO_2-AC_3 electrode. Moreover, the liner charge/discharge curves were probably resulted from double layer charge storage mechanism.

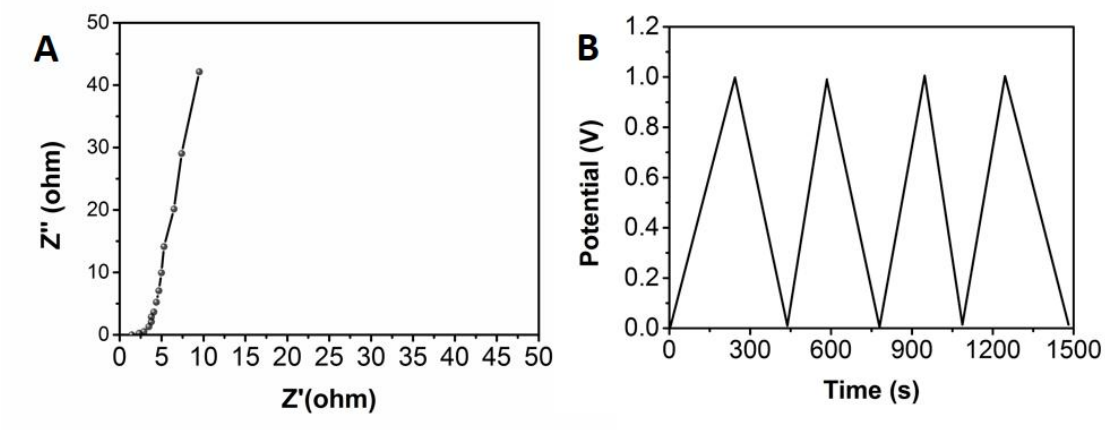

Figure 4. (A) Typical Nyquist plot and (B) galvanostatic charge/discharge curve of MnO_2-AC_3 electrode.

The cycle life of MnO_2-AC_3 electrode is extremely crucial to its industrial application in supercapacitor. Therefore, galvanostatic charge/discharge experiments at the current density of 5 A/g were carried out to evaluate the cycle life of MnO_2-AC_3 electrode. The capacitance retention in function of successive charge/discharge cycles of MnO_2-AC_3 electrode was shown in Fig. 5. The specific capacitance showed a slightly decrease during 1000 successive charge/discharge cycles. However, more than 92% of initial specific capacitance of MnO_2-AC_3 electrode was remained. The observed high stability of MnO_2-AC_3 electrode can be ascribed to the strong interaction between MnO_2 and AC substrate. In general, MnO_2-AC_3 electrode was demonstrated to be very promising in the application of constructing high-performance supercapacitor.

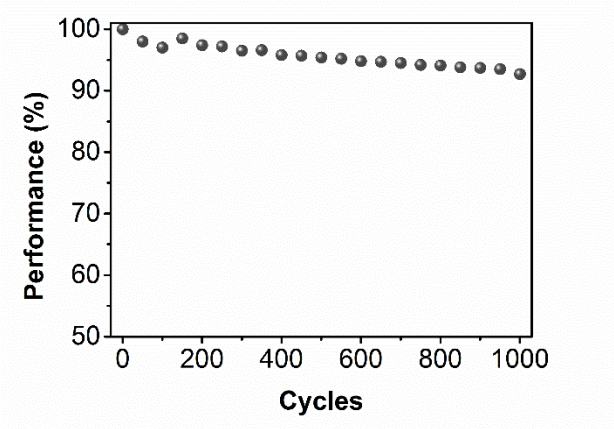

Figure 5. Cycle life of MnO_2-AC_3 electrode during successive charge/discharge cycles.

4. CONCLUSION

Activated porous carbon (AC) was successfully prepared by the carbonization and alkali activation of paulownia flower. Manganese dioxide nanostructures were then electrochemically

deposited on the surface of as-prepared activated porous carbon. The electrode fabricated with MnO_2-AC_3 composite demonstrated remarkable capacitive behavior and excellent stability as well, making MnO_2-AC_3 promising material with potential application in supercapacitor.

ACKNOWLEDGMENTS
This work was supported by Technology Development Program of Shandong Province (2014GGH202003); Natural Science Foundation of Shandong Province (ZR2014JL029) and Technology Development Program of WeiFang City (20121311).

References

1. J.R. Miller and P. Simon, *Science Magazine*, 321 (2008) 651
2. H. Wang and H. Dai, *Chemical Society Reviews*, 42 (2013) 3088
3. C. Liu, F. Li, L.P. Ma and H.M. Cheng, *Adv. Mater.*, 22 (2010)
4. A. Izadi-Najafabadi, S. Yasuda, K. Kobashi, T. Yamada, D.N. Futaba, H. Hatori, M. Yumura, S. Iijima and K. Hata, *Adv. Mater.*, 22 (2010)
5. M. Inagaki, H. Konno and O. Tanaike, *Journal of Power Sources*, 195 (2010) 7880
6. P. Simon and Y. Gogotsi, *Nature materials*, 7 (2008) 845
7. Y. Li, Z. Li and P.K. Shen, *Adv. Mater.*, 25 (2013) 2474
8. X. Yang, C. Cheng, Y. Wang, L. Qiu and D. Li, *Science*, 341 (2013) 534
9. Y. Zhu, S. Murali, M.D. Stoller, K. Ganesh, W. Cai, P.J. Ferreira, A. Pirkle, R.M. Wallace, K.A. Cychosz and M. Thommes, *Science*, 332 (2011) 1537
10. S. Han, D. Wu, S. Li, F. Zhang and X. Feng, *Adv. Mater.*, 26 (2014) 849
11. M. Kaempgen, C.K. Chan, J. Ma, Y. Cui and G. Gruner, *Nano letters*, 9 (2009) 1872
12. Y. Ren, C. Sun, K. Li, L. Wang and M. Song, *Ceram. Int.*, 42 (2015) 1339
13. R. Yang and G. Lian, *Journal of the American Ceramic Society*, 93 (2010) 3560
14. Y. Ren, L. Gao, J. Sun, Y. Liu and X. Xie, *Ceram. Int.*, 38 (2012) 875
15. L. Wang, C. Mccleese, A. Kovalsky, Y. Zhao and C. Burda, *Journal of the American Chemical Society*, 136 (2014) 12205
16. X. Li, X. Zang, Z. Li, X. Li, P. Li, P. Sun, X. Lee, R. Zhang, Z. Huang and K. Wang, *Adv Funct Mater*, 23 (2013) 4862
17. M. Kotal and A.K. Bhowmick, *J Phys Chem C*, 117 (2013) 25865
18. M. Lillo-Ródenas, D. Cazorla-Amorós and A. Linares-Solano, *Carbon*, 41 (2003) 267
19. T.-H. Liou, *Chem. Eng. J.*, 158 (2010) 129
20. C. Peng, X.-b. Yan, R.-t. Wang, J.-w. Lang, Y.-j. Ou and Q.-j. Xue, *Electrochimica Acta*, 87 (2013) 401
21. X. Li, W. Xing, S. Zhuo, J. Zhou, F. Li, S.-Z. Qiao and G.-Q. Lu, *Bioresource technology*, 102 (2011) 1118
22. X.-L. Wu, T. Wen, H.-L. Guo, S. Yang, X. Wang and A.-W. Xu, *ACS nano*, 7 (2013) 3589
23. S.-h. Du, L.-q. Wang, X.-t. Fu, M.-m. Chen and C.-y. Wang, *Bioresource technology*, 139 (2013) 406
24. T.E. Rufford, D. Hulicova-Jurcakova, K. Khosla, Z. Zhu and G.Q. Lu, *Journal of Power Sources*, 195 (2010) 912
25. Q. Wang, J. Yan, Y. Wang, T. Wei, M. Zhang, X. Jing and Z. Fan, *Carbon*, 67 (2014) 119
26. E. Frackowiak, *Phys Chem Chem Phys*, 9 (2007) 1774
27. E. Raymundo-Piñero, F. Leroux and F. Béguin, *Adv. Mater.*, 18 (2006) 1877
28. J. Chen, Y. Liu and Y.-P. Shi, *Journal of Analytical Chemistry*, 64 (2009) 282

29. X. Li, P. Zhang, W. Duan, D. Zhang and C. Li, *Zhong yao cai= Zhongyaocai= Journal of Chinese medicinal materials*, 32 (2009) 1227
30. A. Cross, A. Morel, A. Cormie, T. Hollenkamp and S. Donne, *Journal of Power Sources*, 196 (2011) 7847
31. W.Z. Teo, A. Ambrosi and M. Pumera, *Electrochemistry Communications*, 28 (2013) 51
32. M.-S. Wu, Z.-S. Guo and J.-J. Jow, *J Phys Chem C*, 114 (2010) 21861
33. J. Ma, Q. Cheng, V. Pavlinek, P. Saha and C. Li, *New J Chem*, 37 (2013) 722
34. W. Wei, X. Cui, W. Chen and D.G. Ivey, *Journal of Power Sources*, 186 (2009) 543
35. G. Xiong, K. Hembram, R. Reifenberger and T.S. Fisher, *Journal of Power Sources*, 227 (2013) 254
36. M. Toupin, T. Brousse and D. Bélanger, *Chemistry of Materials*, 16 (2004) 3184
37. J.-G. Wang, Y. Yang, Z.-H. Huang and F. Kang, *Mater. Chem. Phys.*, 140 (2013) 643
38. F. Cataldo, M.V. Putz, O. Ursini and G. Angelini, *Fullerenes, Nanotubes and Carbon Nanostructures*, 24 (2016) 400
39. A. Kausar, *Fullerenes, Nanotubes and Carbon Nanostructures*, 24 (2016) 391
40. M. Ghorbani and M. Hakimi-Nezhaad, *Fullerenes, Nanotubes and Carbon Nanostructures*, 24 (2016) 385
41. A. Safavi, S. Kazemi and H. Kazemi, *Electrochimica Acta*, 56 (2011) 9191
42. Awitdrus, M. Deraman, I.A. Talib, R. Farma, R. Omar, M.M. Ishak, E. Taer, B.N.M. Dolah, N.H. Basri and N.S.M. Nor, 1656 (2015) 11
43. Z.Y. Sui, Y.N. Meng, P.W. Xiao, Z.Q. Zhao, Z.X. Wei and B.H. Han, *ACS applied materials & interfaces*, 7 (2015) 1431
44. S. Gharehkhani, S.F.S. Shirazi, S.P. Jahromi, M. Sookhakian, S. Baradaran, H. Yarmand, A.A. Oshkour, S.N. Kazi and J.B. Wan, *Rsc Advances*, 5 (2015) 40505
45. Y. Zhao, M. Liu, X. Deng, L. Miao, P.K. Tripathi, X. Ma, D. Zhu, Z. Xu, Z. Hao and L. Gan, *Electrochimica Acta*, 153 (2015) 448
46. Z. Yu, L. Tetard, L. Zhai and J. Thomas, *Energy & Environmental Science*, 8 (2015) 702
47. O. Mykhailiv, M. Imierska, M. Petelczyc, L. Echegoyen and M.E. Plonska-Brzezinska, *Chemistry*, 21 (2015) 5783